JTTEE5 9:191-197

Failure of Physical Vapor Deposition/ Plasma-Sprayed Thermal Barrier Coatings during Thermal Cycling

V. Teixeira, M. Andritschky, H. Gruhn, W. Malléner, H.P. Buchkremer, and D. Stöver

(Submitted 1 August 1996; in revised form 1 January 2000)

ZrO_2-7 wt.% Y_2O_3 plasma-sprayed (PS) coatings were applied on high-temperature Ni-based alloys precoated by physical vapor deposition with a thin, dense, stabilized zirconia coating (PVD bond coat). The PS coatings were applied by atmospheric plasma spraying (APS) and inert gas plasma spraying (IPS) at 2 bar for different substrate temperatures. The thermal barrier coatings (TBCs) were tested by furnace isothermal cycling and flame thermal cycling at maximum temperatures between 1000 and 1150 °C. The temperature gradients within the duplex PVD/PS thermal barrier coatings during the thermal cycling process were modeled using an unsteady heat transfer program. This modeling enables calculation of the transient thermal strains and stresses, which contributes to a better understanding of the failure mechanisms of the TBC during thermal cycling. The adherence and failure modes of these coating systems were experimentally studied during the high-temperature testing. The TBC failure mechanism during thermal cycling is discussed in light of coating transient stresses and substrate oxidation.

Keywords zirconia coatings, plasma spraying, sputtering, stress modeling, TBC, failure mechanisms, thermal cycling

1. Introduction

Ceramic coatings are used as protective coatings for engine metal components to improve performance, *e.g.*, thermal barrier coatings (TBCs) deposited by plasma spraying or PVD techniques are currently applied on gas turbine blades and diesel engine components.[1,2]

Conventional TBCs consist of metallic bond coating (typically MCrAlY applied by vacuum plasma spraying or PVD) and a thick ceramic topcoat (typically stabilized ZrO_2 deposited by atmospheric plasma spraying (APS) or by electron beam evaporation). The MCrAlY coat was replaced with a thinner, dense ceramic coating (yttria stabilized zirconia) deposited by direct current (DC) reactive magnetron sputtering (PVD bond coat, see Fig. 1).[3,4] Despite their columnar microstructure, thin PVD coatings can be dense and may act as an efficient diffusion gas barrier at high temperatures to control the oxidation of a metallic substrate, and the columnar structure guarantees an improved strain and stress tolerance. The concept of this TBC coating design is to improve the oxidation and corrosion resistance of the metallic substrate at high temperature. The TBC weight reduction achieved by this fully ceramic duplex TBC with the thinner PVD bond coating is an important aspect, especially for an improved efficiency in rotatory parts in industrial gas turbines. Thermal stress within the coatings occurs due to a mismatch between the thermal expansion coefficients of metallic substrate and coating and due to transient thermal gradients during rapid thermal cycling.[5,6,7] Depending on deposition conditions, the PVD deposition technique may also induce some stress within the coating, which is generally called intrinsic stress. Previous studies showed that this intrinsic compressive stress of the sputtered bond coating may act as a "prestress," which diminishes coating failure due to tensile thermal stresses at elevated temperatures.[6,7] Also the plasma spray process induces some residual stress due to substrate heating during the deposition. Thermal residual stress (usually compressive stress) then develops during cooling to room temperature.

Failure of the TBCs at working conditions is generally attributed to (1) stress developing during cooling after high-temperature exposure and (2) transient thermal stress during rapid thermal cycling.[1,5] In the first case, failure probability is enhanced by oxide scales, growing at high temperatures in a stress free state. In the latter case, compressive stress experienced by the plasma-sprayed (PS) coat may cause the spalling (delamination) of individual lamellae. In any case, the PS coat does not support high tensile stresses and relaxes by microcracking within the lamellar structure. Rather than being a nuisance, the coating toughness is increased by this microcracking and no macroscopic failure is observed even at high working temperatures.

In this contribution, the thermomechanical stability of PVD/PS systems at high temperature was studied. The thermal residual stress developed in the PS top coating during spraying was simulated by using a heat transfer finite element model (FEM) program and an elasto-plastic biaxial stress model, which calculates the stress gradients in the coating/substrate system.[8,9] This computer code has already proved to simulate successfully the experimental measured stresses in PS coatings.[8–11] The thermal stress of the coating during slow and rapid thermal cycling is then calculated by a modified model, taking into account the residual stress due to the deposition technique of the PVD and PS

V. Teixeira and **M. Andritschky,** Physics Department, University of Minho, P-4700 Braga, Portugal; and **H. Gruhn, W. Malléner, H.P. Buchkremer,** and **D. Stöver,** Forschungszentrum Julich GmbH, IWV-2, Institute for Materials and Processes in Energy Systems, D-52425 Julich, Germany. Corresponding author e-mail: vasco@fisica.uminho.pt

coating and the presence of the growing oxide scale. The coating failure mode is discussed by comparing the numerical modeling of the temperature distribution and strain/stress gradients, within TBCs during thermal cycling,[5,10] with experimental data.

2. Experimental Details

2.1 Sample Preparation

Inconel 617 alloy (INCO Alloys International, Inc., Huntington, WV) was used as the substrate material for this study. Grit-blasted (using alumina as the erodent) and polished (SiC P220 grit) substrates were ultrasonically cleaned in acetone and then placed into a high vacuum chamber for the deposition of PVD bond coatings. The substrates were *in situ* sputter cleaned prior to the coating deposition. The PVD bond coating consists of a thin (7 μm) ZrO_2-7 wt.% Y_2O_3 deposited by reactive magnetron sputtering. A 300 μm ZrO_2-7 wt.% Y_2O_3 thick top coat was then deposited on top of the PVD bond coat in a Plasma Technik spraying unit. The deposition was performed, typically at a gun power of about 48 kW, at atmospheric pressure (APS coatings) or in an inert gas atmosphere of 2 bar. Stabilized zirconia powder with a mesh of –45/+10 μm and with a chemical composition of 7.52 wt.% Y_2O_3 (ZrO_2 balance) was used. Details on the deposition conditions, both for the PVD and the PS coating, can be found in Ref 3, and 12.

Three series of duplex coatings were prepared at substrate temperatures of 500, 700, and 900 K for both APS and inert plasma spray (IPS) spraying techniques. Figure 2 shows the cross section of a duplex coating, which has undergone thermal cycling test after the deposition process.

2.2 Coating Testing and Analysis

The PVD bond coatings and sprayed top coatings were, directly after the deposition process, tested by isothermal cycling in a furnace and rapid thermal cycling with a natural gas-oxygen torch. The isothermal cycling consisted of 10 min heatup from 200 °C to maximum temperature and 45 min holding time, at 1000, 1100, and 1150 °C, respectively, followed by cooling down within 10 min with static air. The rapid thermal cycling with the natural gas-oxygen flame consisted of heating up to 1000, 1100, and 1150 °C within 1 min and then cooling down to about 200 °C within 1 min by forced air. The temperature was measured by a thermocouple clamped into a bore hole within the metallic substrate. The failure of the TBC was defined in terms of cracking or spalling/delamination of the zirconia coating within at least 20% of the sample area. This degradation was generally observed during the cooling cycle.

After the thermal treatment, the samples were examined by optical microscopy, scanning electron microscopy, energy dispersive X-ray spectroscopy (EDX), and X-ray diffraction analysis (XRD). The coating adherence of all samples was investigated by pull tests. A pin was glued to the coating surface and cured in a furnace and then a tensile stress was applied until failure.

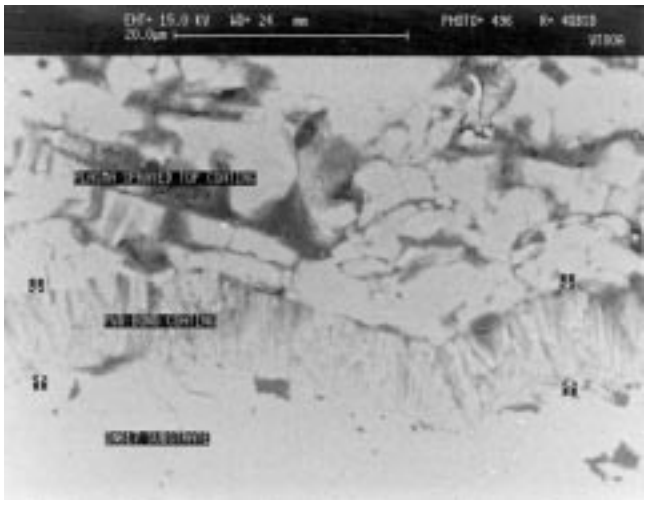

Fig. 1 Micrograph of a typical duplex TBC produced by combination of PVD and PS techniques

3. Numerical and Experimental Results

3.1 Stress Modeling of PVD/PS Duplex Coatings

The as-deposited PVD coating was in a state of intrinsic compressive stress[6,7] as determined experimentally. The as-deposited coating residual stress in the APS and IPS coating was calculated using a numerical FEM code[8,9,10] by a two-step procedure: (1) the temperature within the coating and substrate was calculated and compared with experimental data (Fig. 3); and (2) the coating thermal stress was computed from the temperature gradients, assuming a Young's modulus of about 80 GPa[9,11,13] for the PVD, APS, and IPS coating (Fig. 4). The residual stress near the surface of the top coating was verified experimentally by XRD for the as-deposited samples with and without PVD bond coating.[9,11]

The simulation of the thermal stress of the coating during thermal cycling was performed by solving the unsteady heat conduction equation by an implicit finite difference algorithm, with isotropic and temperature-dependent physical properties. This thermal modeling enabled calculation of the thermal strain and stress fields by an elastic biaxial model, considering also the oxide layer grown at the PVD/substrate interface during the high-temperature exposure.[5,11] The residual stress, as determined experimentally and numerically for the as-deposited multilayer coatings, was then superimposed on the computed stress during thermal cycling. The material parameters used for the simulations are shown in Table 1.

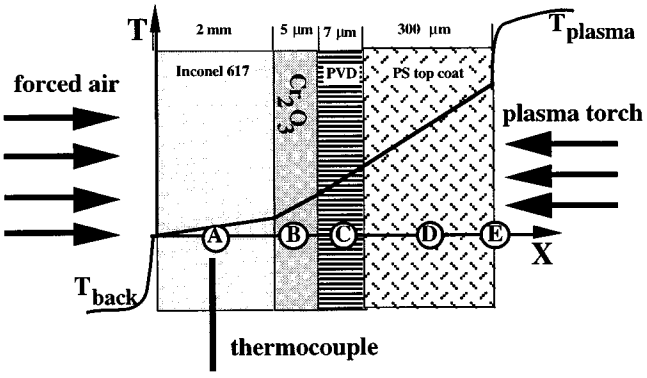

Fig. 2 Cross section of an Inconel substrate coated by a duplex PVD/PS coating undergoing rapid thermal cycling (heating and cooling are done alternatively). Node coordinates indicated by A, B, C, D, and E are the model points in Fig. 4, 5, and 9

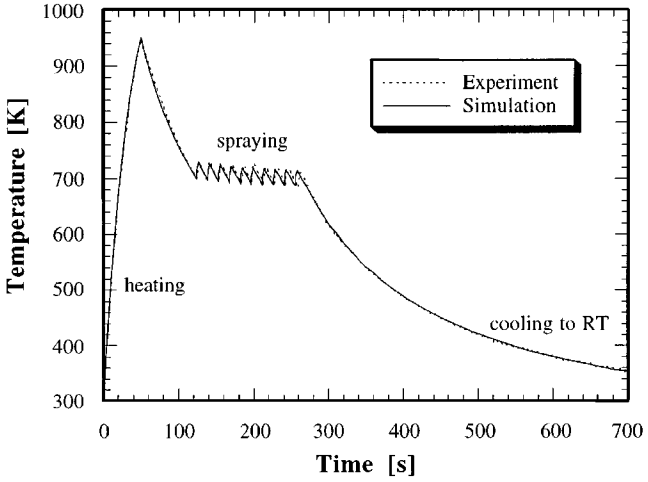

Fig. 3 Simulated and measured temperature evolution during plasma spraying deposition of zirconia top coating (at point A as defined in Fig. 2)

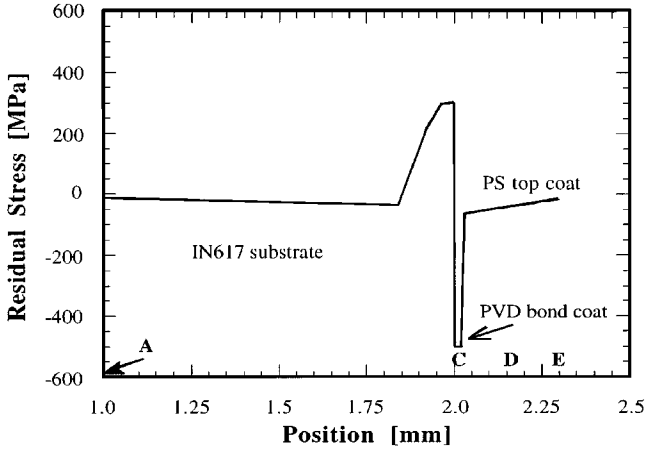

Fig. 4 Numerical simulation of the residual stress in PVD/PS TBC after deposition. The distance is measured from the uncoated surface of the coating. The points A, B, C, D, and E correspond to the respective points in Fig. 2, 5, and 9

Table 1 Physical properties (at room temperature) used in the heat transfer and stress simulations

Physical property	Substrate IN 617	Chromia layer	PVD bond coat	PS top coating
Density (g/cm^3)	8230	5210	5700	5700
Thermal conductivity (W/m/K)	13.4	1.2	1.8	1.8
Heat capacity (J/kg/K)	419	814.9	450	450
Emissivity	0.5	0.7	0.8	0.8
Young's modulus (GPa)	215	265	82	82
Poisson ratio	0.288	0.294	0.23	0.23
Thermal expansion coefficient (10^{-6}/K)	12	8.68	8.6	8.6
Yield stress, Rp0.2% (MPa)	360	300	138	138

3.2 Isothermal Cycling

During isothermal cycling, one has to discuss separately the coating stress in the three layers: (1) the growing Cr_2O_3 oxide layer, (2) the PVD layer, and (3) the PS top coat. The Cr_2O_3 layer grows, between the PVD layer and the metallic substrate, by oxygen diffusion through the PVD layer. We assume that the volume increase due to the oxidation of the chromium is relatively low and, therefore, the Cr_2O_3 layer is stress free at the growth temperature. During the cooling cycle, a compressive stress develops within the Cr_2O_3 layer due to the mismatch in thermal expansion coefficient of the coating and the substrate. The PVD layer is in a state of intrinsic compressive stress at room temperature due to the deposition procedure.[7] This compressive stress is balanced by the tensile thermal stress when heating the sample. At working conditions, the PVD coating is therefore almost in a stress-free condition.

The PS top coating is in a tensile stress at working temperatures of 1000 and 1150 °C. During the heat treatment, it is assumed that the coating relaxes almost immediately, by microcracking, to a tensile stress level of about 140 MPa (Table 1), and during prolonged heat treatment, the thermal stress is canceled by creep within the coating and eventually within the substrate.[14] Microcracking for ceramic coatings undergoing thermal cycling was detected by acoustic methods by other authors, which confirmed the model assumptions of the current research.[15] Due to this stress relaxation at high temperature, a compressive thermal stress is then again generated within the coating during the cooling procedure (Fig. 5). The compressive residual stress of about −300 MPa at room temperature, after about 300 thermal cycles, within the upper layer of the PS coating was also verified experimentally by XRD measurements. A value of about-250 MPa for a coating subjected to thermal cycling was found, which is in good agreement with the numerical results.[11] Table 2 presents some stress calculations and the correspondent measurements for as-deposited and thermal cycled coatings.

Coating failure during isothermal cycling occurred generally at the interface of substrate and PVD coating within the growing Cr_2O_3 layer. The XRD and EDX analyses identified this oxide layer as α-Cr_2O_3. No spinel or other oxides were present, which eventually could lower the adherence of the PVD coating.[12] At 1000 °C, the coatings resisted up to 300 cycles, without any failure (Fig. 6 and 7), regardless of deposition conditions and substrate preparation (polishing or sand blasting).

Although it is known that Cr_2O_3 layers tend to deteriorate significantly at temperatures above 1050 °C, higher temperatures were applied to accelerate the coatings degradation. At 1100 and 1150 °C, the IPS coatings failed generally at lower cycle numbers than the APS coatings. Furthermore, sand-blasted surfaces, although they showed higher oxidation rates, failed later than polished surfaces, probably due to a mechanical interlocking effect. The lifetime of the APS coatings deposited at 500, 700, and 900 K seems to be similar during isothermal cycling at 1100 and 1150 °C. However, for this test, some coatings, such as APS coatings deposited at 500 K on sand-blasted substrates (*i.e.*, with a lower prestress due to the deposition procedure), exhibited a higher average lifetime (Fig. 7).

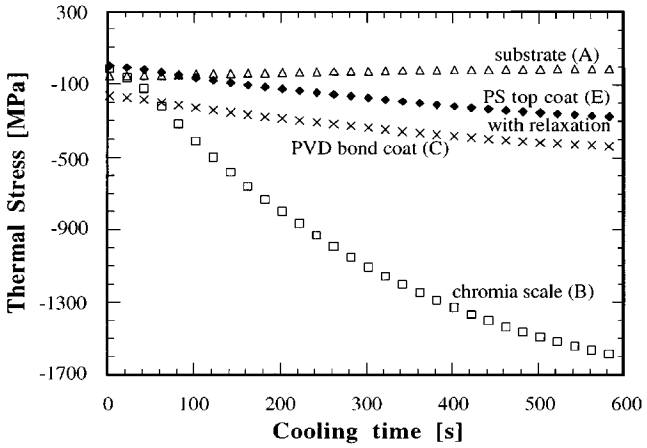

Fig. 5 Thermal stress at the positions A (substrate), B (chromia scale), C (PVD bond coat), D (center of the PS top coat), and E (surface of the PS top coat) during the cooling phase of the isothermal cycling (cooling time is 600 s and temperature decreases linearly from 1100 to 200 °C). The values indicated by "with relaxation" correspond to the stress in the top coat, admitting cancellation of the stress in the top coat due to high-temperature creep of the Inconel substrate

Table 2 Residual stress in the PS top coating surface for as-deposited and thermal cycled state of duplex PVD/PS TBCs as determined by XRD and by stress modeling

State of the coating	Coating code (a)	Model calculation (MPa)	XRD (MPa)
As- deposited	APS-sbl5	52	38
As- deposited	APS-sbl7	12	10
As-deposited	APS-sbl9	–5	–17
As-deposited	IPS-sbl9	–5	–25
After isothermal cycling at 1100 °C	APS-sbl5	–280	–240
After rapid thermal cycling at 1000 °C	APS-sbl7	–120	–71
After thermal cycling	Cr2O3	-1800	-2060

(a) APS-sbl5, APS-sbl7, IPS-sbl9, *etc*. mean the mode of deposition of the Zr_2O_3-7 wt.% Y_2O_3 top coat (*e.g*., APS-sbl5 is an atmospheric PS zirconia coating deposited at 500 K on a sand-blasted substrate, IPS-sbl9 is a high pressure plasma spraying coating deposited at 900 K on a sand-blasted susbstrate. *etc*.)

Nevertheless, PS coatings deposited at higher substrate temperatures showed greater pull strength even after prolonged thermal cycling. Figure 8 shows the pull strength data measured within the undamaged area of the coatings after thermal cycling and, as well, in the as-deposited state.

During the pull test, all coatings exhibited cohesive failure within the PS top coating. The greatest cohesive strength of the PS coatings was found for APS coatings deposited at high substrate temperatures. As the substrate temperature decreased, the cohesive strength of the lamellae diminished from 46 to 22 MPa, and as the chamber pressure increased during the deposition (IPS coatings), cohesive strength decreased. The cohesive strength of the lamellae is in any case lower than the adhesive strength of the PVD coating both in the as-deposited form and after thermal cycling (see also Ref 3 and 4).

Tests with single PVD layers on the substrate[4] also revealed the cohesive strength of the chromia layer to be about 45 MPa. The

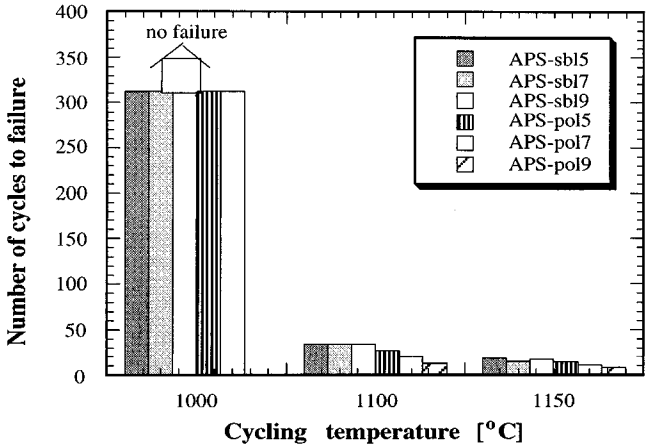

Fig. 6 Coating lifetimes in isothermal cycled duplex PVD/PS coatings for different temperatures of cycling and for different deposition temperatures. (APS-pol5 indicates polished substrate coated with PVD bond coating and APS top coat deposited at 500 K, APS-sbl7 indicates sand-blasted substrate coated with PVD bond coating and APS top coat deposited at 700 K, *etc*.)

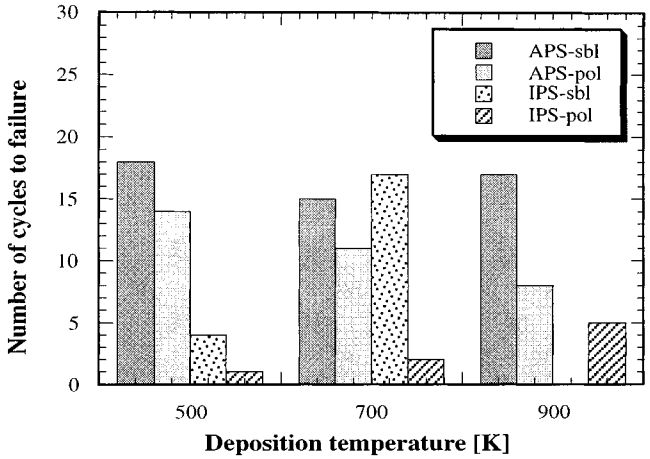

Fig. 7 Comparison between PVD/APS and PVD/IPS coating systems tested in furnace cycling at 1150 °C. (APS-sbl indicates sand-blasted substrate coated with PVD bond coating and APS top coat, APS-pol indicates polished substrate coated with PVD bond coating and APS top coat, IPS-sbl indicates sand-blasted substrate coated with PVD bond coating and IPS top coat, and IPS-pol indicates polished substrate coated with PVD bond coating and IPS top coat.)

cohesive strength of the PVD layer is always higher (>65 MPa, which corresponds to the adhesive strength of the PVD layer on the substrate) than the strength of the Cr_2O_3, or the PS coatings.[4]

3.3 Rapid Thermal Cycling

During rapid thermal cycling by alternatively heating the coating surface with a plasma torch and cooling the substrate surface using forced air, the temperature and stress distribution within the coating/substrate system were somewhat different compared to the temperature distribution during isothermal cycling in a furnace (see Fig. 9). Total stress relaxation due to creep would not happen during the short period at maximum temperature, and the model calculations for the stress within the PS top

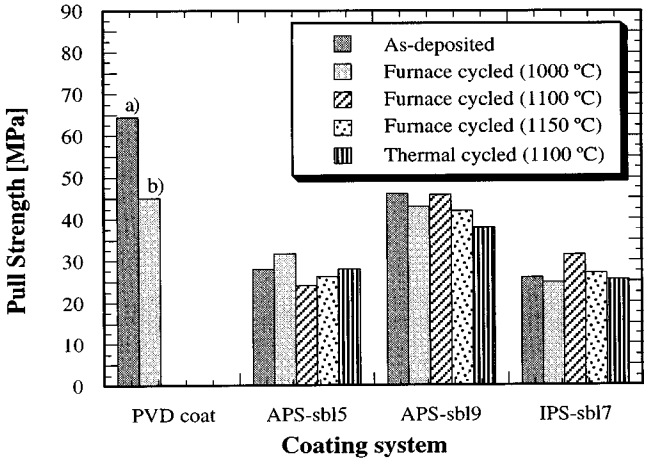

Fig. 8 Pull strength data for the duplex TBCs as-deposited, isothermal cycled at 1000 °C (after 310 cycles), isothermal cycled at 1100 °C (34 cycles), isothermal cycled at 1150 °C (17 cycles), and after rapid thermal cycling at 1100 °C (450 cycles). The failure was cohesive within the PS coat if not labeled otherwise by (a) adhesive at the PVD-substrate interface or (b) cohesive within chromia scale. (APS-sbl5 indicates sand-blasted substrate coated with PVD bond coating and APS top coat deposited at 500 K, APS-sbl9 indicates sand-blasted substrate coated with PVD bond coating and APS top coat deposited at 900 K, and IPS-sbl7 indicates sand-blasted substrate coated with PVD bond coating and IPS top coat deposited at 700 K.)

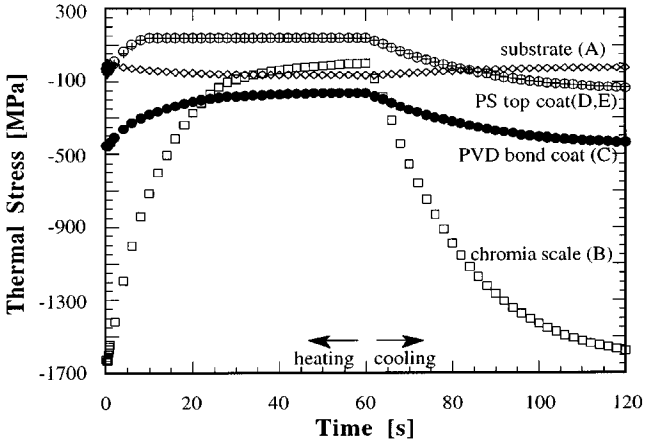

Fig. 9 Numerical model results for coating stress evolution during one thermal cycle (cooling and heating periods correspond to 200 °C as minimum substrate temperature and 1100 °C as maximum)

coat after cooling to room temperature indicated a compressive stress of about −100 MPa. These calculations considered solely the stress relaxation due to microcracking. Nevertheless, the numerical result showed that the differences in the thermal stress at maximum and minimum temperatures between isothermal cycling and rapid thermal cycling are not significant.

During the relative short time at maximum temperature (about 30 s · 650 cycles = 5.5 h at T · 1000 °C), only a relatively thin Cr_2O_3 layer builds up. An oxide layer of the corresponding thickness did not cause coating failure during isothermal cycling. The duplex coatings satisfactorily resisted rapid thermal cycling from room temperature to 1000 and 1100 °C within the maximum number of cycles studied (650 and 450 cycles, respectively). Also, the pull tests performed after the rapid cycling did not show any significant differences (Fig. 8) from the results obtained from isothermal cycling. Therefore, it is expected that the duplex coatings will not fail during thermal cycling.

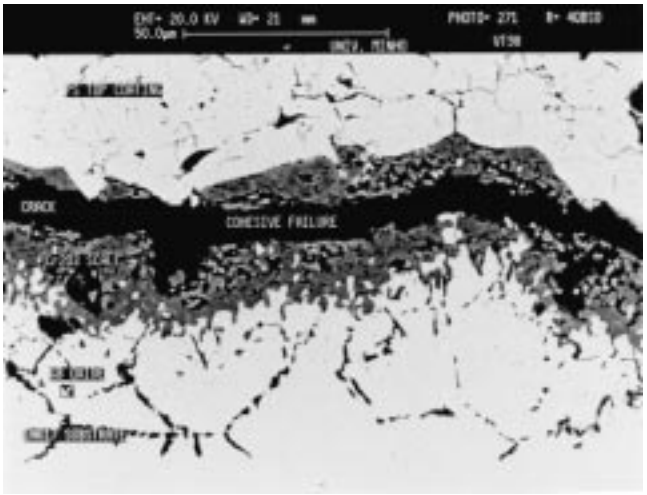

Fig. 10 Crack propagation within the chromia scale (typical cohesive failure) for the duplex PVD/PS coatings undergoing furnace cycling

Nevertheless, during thermal cycling up to the maximum temperature (1150 °C), a few samples exhibited spalling of individual lamellae of the PS top coating surface. A detailed stress analysis of the first few seconds of the heating cycle predicted additional compressive stress at the surface of the top coat, which may be responsible for this additional failure mode.[11]

4. Discussion

Numerical simulations of the thermal stress generated in TBCs (consisting of a thick (300 μm) PS YSZ top coat and a relatively thin (7 μm) YSZ bond coat, deposited by PVD on an Inconel 617 substrate), taking into account the intrinsic stress, revealed that the main stress occurs within the growing oxide layer. Experimental results confirm that failure occurs within these oxide layers (Fig. 10). Neither the numerical stress analysis nor the experimental data reveals a significant difference between isothermal cycling and rapid thermal cycling (heating and cooling rates about 1 and 18 K/s, respectively).

The thermal compressive stress leads to generation of cracks parallel to the surface[16,17,18] starting at pre-existing flaws or microcracks. During continued thermal cycling, these cracks may propagate cycle by cycle, leading to spalling or complete delamination. In fact, the failure was observed during the cooling period and the location of delamination was for all coatings almost within the chromia scale grown during the high-temperature exposure. The fracture path remains within the Cr_2O_3 layer in the current experiments. This finding is different from the literature. For traditional TBCs produced by plasma spraying, it is reported[18,19,20] that the fracture path initiates in the region of the oxidation product and continues "cutting" through the PS top coat, as illustrated in Fig. 11. However, for TBCs produced by electron beam evaporation (EB-PVD) the location of the failure is at the interface of alumina and bond coat.[21] (See Ref 22 to 24

for a detailed analysis of stress fields and crack growth in rough substrates.) In traditional TBCs, the oxidation product is mainly αAl_2O_3, which has a lower oxidation rate, but due to the relatively high Young's modulus, a higher compressive stress develops during cooling. Due to the different mechanical properties of the oxidation product (Cr_2O_3 and Al_2O_3) and the adjacent layer (YSZ-PVD coating and YSZ-PS coating, respectively), the crack, in one case, deflected at the interface between the two layers and, in the other case, propagated across the two layers (see Ref 16 and 24 for the propagation of cracks along an interface region).

The failure analysis for isothermal cycling at different temperatures indicates that the most probable coating life-limiting factors are thickness of the grown oxide scale, thermal stresses, plastic deformation of substrate, irregularities of the interface, and, of course, adherence of the coatings on the substrate. Although the parabolic oxidation constant for alloys that form alumina at high temperature is lower than that for the "chromia" forming alloys,[4,18] it is believed that the oxide thickness is not the main critical factor. The thermal stress, which depends on the Young's modulus of the grown oxide, also plays an important role. The crack path and the eventual deflection of the crack at interfaces and irregularities are also important factors. In summary, the coating lifetimes obtained using a chromia forming base material and substituting the thick VPS metallic bond coat by a thin PVD ceramic bond coat are similar to traditional TBCs.[12,17] In corrosive atmospheres with agents such as sulfur, where Cr_2O_3 has shown good protective properties, the suppression of the Al_2O_3 layer might even be more valuable.[12]

Creep mechanisms and the periodical stress relief at wavy interfaces are certainly factors to be considered.[20,21] Further modeling work for the PVD/PS TBCs during thermal cycling will consider two-dimensional/three-dimensional FEM analysis and include some important effects such as the irregularities of the interface, creep mechanisms, and fracture mechanics of the substrate and of the three layers within the multilaminar coating.

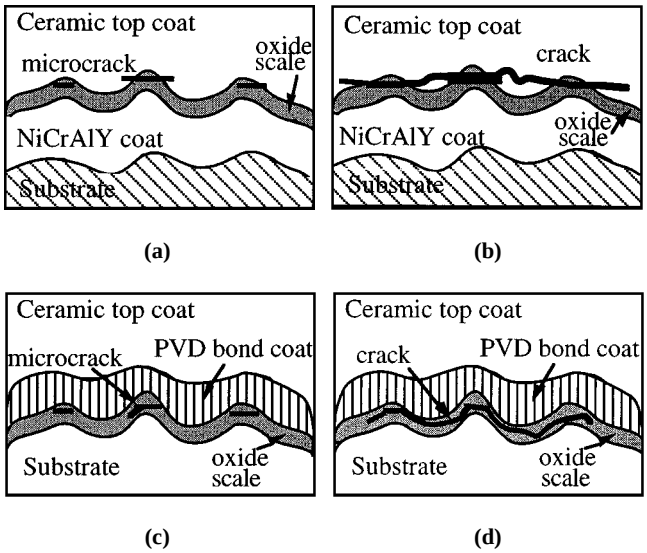

Fig. 11 (**a**) Schematic diagram of oxidation and microcrack growth for the traditional TBC; (**b**) crack propagation along the lamellar interfaces; (**c**) schematic of the oxidation in substrate/PVD interface, illustrating the crack growth at the asperities of the rough substrate; and (**d**) crack propagation along the less tough material (the chromia scale)

5. Conclusions

A TBC system based on duplex PVD-PS ceramic coatings was produced and tested at high temperatures. The TBC consists of a ZrO_2-7 wt.% Y_2O_3 PS top coat applied on Inconel 617 previously coated with a thin dense stabilized zirconia coating produced by the PVD technique. The adherence and failure modes of these coating systems were studied during high-temperature cyclic tests (furnace cycling and flame thermal cycling). The coating lifetimes obtained using Inconel 617 (a chromia forming base material) and replacing the thick VPS metallic bond coat (MCrAlY, which is an alumina forming material) by a thin PVD ceramic bond coat are similar to the conventional TBCs.

The residual stress for the as-deposited coatings were determined by a FEM computer code developed for the simulation of the plasma spraying process, and the results showed that the level of stress at the surface was significantly low (–20 to 40 MPa depending on deposition temperature and coating thickness), in good agreement with XRD measurements. The as-deposited coatings showed a linear stress gradient with a higher compressive stress at the interface and a significantly low stress level at the surface. The temperature gradients within the duplex PVD/PS TBCs during the thermal cycling process were numerically modeled using a heat transfer program, and the corresponding coating stress distributions were calculated using a biaxial elasto-plastic stress model. After the heat treatment, the top coating developed a higher compressive stress on cooling due to the relaxation processes at high temperature. The stress model presented–300 MPa, which agreed with the experimental measurement (about –250 MPa).

The coatings applied on grit-blasted substrate surfaces with the PVD bond layer exhibited higher lifetimes compared to those deposited on smooth substrates. During furnace cycling, failure occurred within the grown oxide due to an excessive in-plane compressive stress during the slow cooling process, which is also related to the increase of the oxide thickness. This compressive stress generated tensile stress normal to the interface and was responsible for the observed microcrack propagation parallel to the interface. For isothermal cycling at 1000 °C, the coatings resisted without any observed failure for more than 300 cycles. For thermal cycling with a natural gas-oxygen flame heating to 1000 °C in 1 min and cooling with forced air within the same time, the coatings resisted up to 650 cycles without any failure. The cohesive strength of the PS top coating ranged from about 20 to 45 MPa (depending on coating porosity) and was not altered after prolonged heat treatment such as furnace cycling or flame thermal cycling.

Acknowledgments

The authors are thankful to Dr. Fischer, Forschungszentrum Jülich, for doing the XRD stress analysis. This work is a part of a project partially supported by the German-Portuguese Collaboration (BMFT/JNICT) under Contract No. RFA-423.

References

1. P. Vincenzini: *Ind. Ceram.*, 1990, vol. 10, pp. 113–26.
2. J.T. DeMasi-Marcin and D.K. Gupta: *Surf. Coatings Technol.*, 1994, vol. 68/69, pp. 1–9.
3. V. Teixeira, M. Andritschky, L. Rebouta, H.P. Buchkremer, and D. Stöver: *Proc. 3rd Eur. Congr. on Thermal Plasma Processes—TPP94*, D. Neuschütz, ed., VDI-G. Werkstofftechnik-W, Aachen, Germany, VDI Ber., 1995, vol. 1166, pp. 445–52.
4. M. Andritschky, V. Teixeira, L. Rebouta, H.P. Buchkremer, and D. Stöver: *Surf. Coatings Technol.*, 1995, vol. 76/77, pp. 101–05.
5. V. Teixeira, M. Andritschky, H. Gruhn, W. Malléner, H.P. Buchkremer, and D. Stöver: *Proc. 8th Nat. Thermal Spray Conf.*, Houston, TX, 1995, C.C. Berndt and S. Sampath, eds., ASM International, Materials Park, OH, 1995, pp. 515–20.
6. V. Teixeira and M. Andritschky: *High Temp.-High Pressures*, 1993, vol. 25, pp. 213–19.
7. M. Andritschky and V. Teixeira: *Proc. "Advances in Materials and Processing Technologies—AMPT9311,* M. Hashmi, ed., Dublin University, Dublin, 1993, vol. 2, p. 729; *Vacuum*, 1994, vol. 45, pp. 1047–50.
8. H.J. Groß, W. Malléner, D. Stöver, and R. Vaßen: *Proc. 5th Nat. Thermal Spray Conf.*, Anaheim, CA, 1993, C.C. Berndt and T.F. Bernecki, eds., ASM International, Materials Park, OH, 1993, pp. 581–85.
9. H.J. Groß, W. Fisher, R. Vaßen, W. Malléner, and D. Stöver: *Proc. Thermal Spraying—TS93*, DVS, Aachen, Germany, 1993, p. 52.
10. H. Gruhn, W. Malléner, and D. Stöver: *Proc. 8th Nat. Thermal Spray Conf.*, Houston, TX, 1995, C.C Berndt and S. Sampath, eds., ASM International, Materials Park, OH, 1995, pp. 231–36.
11. V. Teixeira, M. Andritschky, W. Fischer, and D. Stöver: in *Advanced Multilayered and Fibre-Reinforced Composites—Problems and Prospect*, Y.M. Haddad, ed., Kluwer Academic Publ., Series E-Applied Sciences, 1998, vol. 3/43, pp. 415-30.
12. Andritschky, L. Rebouta, and V. Teixeira: *Surf. Coatings Technol.* 1994, vol. 68/69, pp. 81–85.
13. D. Schneider, T. Schwarz, H.P. Buchkremer, and D. Stöver: *Thin Solid Films*, 1993, vol. 224, pp. 177–83.
14. G. Kerkhoff, R. Vaβen, C. Funke, and D. Stöver: *Materials for Advanced Power Engineering 1998*, Proc. 6th Liège COST Conf., J. Lecomte-Beckers, F. Schubert, and P.J. Ennis, eds., Forschungszentrum Jülich, Jülich, Germany, 1998, vol. 5-III, pp. 1669-77.
15. C.C. Berndt: *J. Mater. Sci.*, 1989, vol. 24, pp. 3511–20.
16. M. Schütze: *Mater. Sci. Technol.*, 1988, vol. 4, pp. 407–14.
17. A.G. Evans and J.W. Hutchinson: *Int. J. Solids Struct.*, 1984, vol. 20, pp. 455–66.
18. B.C. Wu: *J. Mater. Sci.*, 1990, vol. 25, pp. 1112–15.
19. S.F. Chang: *J. Vac. Sci. Technol.*, 1991, vol. A9, pp. 2099–2106.
20. R. Miller and C. Lowell: *Thin Solid Films*, 1982, vol. 95, pp. 265–73.
21. E. Lee and R. Sisson: *Proc. 7th Thermal Spray Industrial Applications*, C. Berndt and S. Sampath, eds., Boston, MA, ASM International, Materials Park, OH, 1994, pp. 55–60.
22. G. Chang, W. Phucharoen, and R. Miller: *Surf. Coatings Technol.*, 1987 vol. 30, pp. 13–28.
23. U. Marewski, D. Stöver, and R. Hecker: *Surf. Coatings Technol.*, 1991, vol. 46, pp. 47–54.
24. M.D. Thouless: *J. Vac. Sci. Technol.*, 1991, vol. A9 (4), pp. 2510–16.